# The Effects of Material Combination and Surface Roughness in Lubricated Silicon Nitride/Steel Rolling Contact Fatigue

[a]*J. Kang, [a]M. Hadfield and [b]R. Ahmed

[a]Bournemouth University, Sustainable Product Engineering University Research Centre
School of Design, Engineering & Computing, Studland House, 12 Christchurch Road,
Bournemouth, Dorset, BH1 3NA, UK.
[b]Department of Mechanical and Chemical Engineering, Heroit-Watt University, UK.

**Abstract:** Four kinds of commercially finished 12.7 mm HIPed silicon nitride bearing balls with surface roughness values $R_a$ ranging from 0.002 to 0.016 μm were tested using a four-ball rolling configuration. They were rolling against two types of steel testing balls with different surface roughness and hardness, in fully lubricated condition at a maximum compressive stress of 6.58GPa and at a speed of 10,000 rpm for over 135 million stress cycles. Rolling track surfaces were examined by microscope, SEM, 3-D surface analysis and interference profilometry. Experiment results show that the composite surface roughness are most influential. The shape of the surface topography of silicon nitride are not very sensitive. The slight difference in steel hardness may lead to significant differences in steel fatigue life.

**Key Words:** Engineering ceramics (A); Ferrous metals and alloys (A): Fatigue (E)

---

* Corresponding author

E-mail: jkang@bournemouth.ac.uk

Tel.: +44 (0)1202 503750

Fax: +44 (0)1202 503751

## 1. Introduction

Hybrid precision ball bearings (with advanced ceramic balls as rolling elements, and steel inner and outer rings) are now used extensively in aerospace engineering and precision machine tools because of the thermal resistance, corrosion resistance, low density, high elastic modulus and low friction properties of ceramic rolling elements [1]. Currently most commonly used material for advanced ceramic rolling elements is HIPed (Hot Isostatically Pressed) silicon nitride. Hybrid precision ball bearings are much widely employed than all ceramic bearings. Thus the rolling contact fatigue life between ceramic/steel contact is of great interest.

In practice, the rolling contact fatigue failure of steel raceway very often is the limiting factor in hybrid precision ball bearings. The advanced ceramic rolling elements normally exhibit much better rolling contact fatigue performances. In recent years the rolling contact fatigue life of steel raceway has been greatly increased by various efforts. One effort in the design stage was to increase the ball/raceway conformity in order to reduce the Hertzian contact stresses [2]. Other efforts involved in the manufacturing stage include the surface quality control and surface treatment of steel raceway. No published literature on the effects of the surface hardness and surface roughness of steel in rolling contact with ceramic bearing materials is available. A very early study on the steel/steel contact using a rolling four-ball machine showed that upper balls of the optimum hardness give the best life when running against lower balls of like hardness or slightly increased hardness of up to 10%. Upper balls significantly harder than lower balls appear to cause premature failure of the lower balls [3].

There are many parameters to describe surface roughness, for example, $R_a$ (roughness average), $R_q$, also called RMS (rms) (root-mean-square roughness), $R_t$ (maximum peak to valley height) and $R_{sk}$ (skewness). Among those, $R_a$ is most commonly used to represent surface roughness and $R_q$ is generally considered to be most important in lubricated contact because it defines the composite surface roughness, which determines the lambda ($\lambda$) ratio (under EHD lubrication). With steel, it was reported that surface fatigue depended greatly on $R_q$ [4]. A data-fitted rolling bearing life prediction model revealed that the compiled steel full rolling-bearing life tests showed a consistent downward trend as the composite RMS roughness height increased. This indicated that the mathematical life prediction model, which took the surface roughness into account, underestimated the life-shortening effect of a rougher surface [5].

The relationship between the surface roughness and rolling contact fatigue life of advanced ceramic rolling elements is of great concern. Because these ceramic rolling elements are subjected to high cyclic contact stresses, currently they are finished to the best possible surface roughness value in order to reduce the risk of rolling contact fatigue failure according to experiences with steel rolling elements. The material properties of ceramics are very different from steel, especially with the technological advances of powder manufacture and material densification. This philosophy of obtaining the best possible surface roughness may lead to over-engineering of ceramic rolling elements. The relationship between surface roughness parameters and rolling contact fatigue life are therefore of interests and concerns for both industry and academia.

Lakshminarayanan and Chao studied the lubricated rolling contact of steel/silicon nitride using a ball-on-rod rolling-contact-fatigue (RCF) tester. The as-ground silicon nitride rods ($R_a$ 0.18 $\mu$m) exhibited neither wear nor spalling in the RCF tests, while the ground-

and-lapped silicon nitride rods ($R_a$ 0.08 µm) showed no wear but occasional spalling failure [6]. The rolling contact fatigue performance of ceramic/ceramic contact with different surface roughness was studied by Effner and Woydt [7], and by Westkaemper and Hoffmeister [8] as well, on the twin-disk tribometer. They both reported there was an optimum surface roughness values $R_{VK}$ (reduced valley depth) range. When the surface roughness values $R_{VK}$ was below or higher than this range, the rolling wear increased considerably. Effner and Woydt reported the optimum range is 0.5 µm ≤ $R_{VK}$ ≤ 0.9 µm, whilst for Westkaemper and Hoffmeister, it is 0.3 µm ≤ $R_{VK}$ ≤ 2 µm. The rolling contact fatigue tests on silicon nitride/silicon nitride contact conducted by Chao and Lakshminarayanan showed that the bearing-grade balls ($R_a$ 0.005 µm) rolling on as-ground ($R_a$ 0.18 µm) rods produced a high initial wear rate in both elements that decreased exponentially with time or number of loading cycles. Improving the surface finish on the rods by lapping ($R_a$ 0.05 µm) produced delayed wear in both elements, i.e., the wear rate was initially zero during an incubation period, then increased and finally decreased [9].

This paper presents a recent experimental study on four kinds of commercially finished HIPed silicon nitride rolling elements with surface roughness values $R_a$ ranging from 0.002 to 0.016 µm in rolling contact with two kinds of steel balls with different surface hardness and surface roughness.

## 2. Experimental Procedures

### 2.1 Silicon nitride test samples

Four kinds of HIPed silicon nitride balls with diameters 12.7 mm (½"), commercially finished to grade 5, were procured from different manufacturers, and were designated as A, B, C and D. Table 1 summarises the measured geometric and material properties of testing samples A to D. Surface hardness were measured using a Buehler Hardness Indenter, at a load 10kg, loading time 10 sec and loading speed 100µm/sec. Fig. 1 gives the detailed statistical analysis values for different roughness parameters of testing samples A through D measured by a Talysurf 2D surface profiler, with each sample 3 balls, each ball 3 points. Fig. 2 is the microscopy observation on the surfaces of samples A ~ D before RCF test.

### 2.2 Steel test samples

In this study, the steel test samples were procured from two different suppliers. They were both supplied as standard steel testing balls (specification: 0.5″ ball Reference RB12.7/310995A, material: AISI 52100 bearing steel). The measured geometric and physical properties of the steel testing balls are listed in Table 2. Fig. 3 shows the surface microscopy images of the two kinds of steel balls.

### 2.3 Test machine

Accelerated rolling contact fatigue tests were performed on a Plint TE92 HS 10,000 rev/min Microprocessor Controlled Rotary Tribometer [10]. In this study, it was configured as a high-speed modified four-ball machine according to the Institute of Petroleum

(UK) IP 300 rolling test procedure. Fig 4 is the schematic of the modified four-ball rolling configuration. The upper ball (3) is held in the collet (2) and rotates at the spindle (1) speed. The retainer cup (7) has a race with slightly bigger radius than ½" ball to accommodate three lower balls (4). Oil can be filled full of cup before test, and during testing period oil can be added through a hole in the cup cover (8) to maintain the test in fully lubricated condition. The heater pad (5) in conjunction with a thermocouple ensures that the temperature is above the specified value. When temperature is lower than this specified value, the heater pad will be on. The four-ball rolling kinematics was described by Kruger and Bartz in Chapter 10 of reference [4], the current configuration was categorised as type II machine. The upper ball stress cycle factor L is:

$$L = Z \left[ \frac{R_a + 2R_p}{2(R_a + R_p)} \right] \tag{1}$$

Where Z is the number of lower balls, $R_a$ is the upper ball radius, and $R_p$ is the lower ball radius. In this case, $R_a = R_p = 6.35$mm, Z=3, substitute these figures to equation (1), L=2.25. This means when the spindle rotates one revolution, the upper ball will endure 2.25 stress cycles.

*2.4 Test programme*

Before each test, sample ball were cleaned in an ultrasonic bath by acetone. The lubricant oil for all tests was Shell Talpa 20 with a kinematic viscosity (cSt) 94.6 at 40 °C and 8.8 at 100 °C. The lubricant oil was filled to the retainer cup before the test, and was added every 24 hours during the test. The test load, speed and temperature etc. were recorded in a computer file at pre-set sampling rate during each test. In all tests, temperature setting is 50 °C, so that when start a new test heater pad will be on until the temperature reaches 50 °C. Normally the test is stopped before reaching the setting time due to the failure of one lower steel ball. In this case the retainer cup assembly is taken out and cleaned up, then three new steel balls are fitted and new oil is filled up, and the test is then continued. The failure of the lower steel ball is normally a fatigue spall on the rolling track as shown in Fig. 5. By changing the lower steel balls, the rolling contact stress cycles for the upper silicon nitride ball is assured. After each test, the upper silicon nitride ball was cleaned in an ultrasonic bath by acetone. Microscopy, Scanning Electron Microscope (SEM), interference profilometry and 3D topographic analysis were conducted.

## 3. Experimental Results

A summary of the rolling contact fatigue test records is given in Table 3. The calculated Hertz contact stresses [11] are shown in Table 4. The calculated minimum film thickness ($h_{min}$) and lambda ratio ($\lambda$) are listed in Table 5, using the classical Elastohydrodynamic (EHD) equations developed by Dowson and Higginson [12]. In these tables, A1 denotes silicon nitride A in rolling contact with Type 1 steel balls, and A2 denotes silicon nitride A in rolling contact with Type 2 steel balls, and so on. For silicon nitride C in rolling contact with Type 2 steel balls, three test runs were conducted, and therefore they were denoted as C2-1,

C2-2 and C2-3. In all of the tests, only one silicon nitride ball was failed by a fatigue spall, which is C2-1. Steel balls (Type 1 and Type 2) were constantly failed by fatigue spalls of various sizes, as shown in Fig. 5. These fatigue spalls were comparable in size with the roling track width (diameter of the Hertzian contact circle). The fatigue spall in Fig. 5 (a) is about 700 μm by 500 μm, Whilst in Fig. 5 (b) it is about 380 μm by 250 μm.  When one of the steel balls failed with a fatigue spall, three new steel balls of the same type were fitted, and the time for this kind of change is listed in Table 3 under the column of "Lower steel balls changed after (hours)". Fig. 6 shows the microscopy observations of the rolling tracks of silicon nitride A to D after testing.

*3.1 Silicon nitride A in rolling contact with Type 1 and Type 2 steel balls*

Silicon nitride A are with an average $R_a$ value 0.004 μm and a negative skewness value –1.8, which implies that the bulk material is above the mean line (the surface has more valleys than peaks). After 134.35 hours RCF test (181 million stress cycles) with Type 1 steel balls, no difference can be observed on the rolling track under optical microscope (Fig. 6 A1) except for the oil stain deposited on the outer edge of the rolling track which could not be removed by ultrasonic cleaning. Fig. 7 is the analysis of the rolling track by the 3D surface analyzer. From the Oblique Plot of Fig. 7, slight wear on the rolling track can be seen. The amount of wear is identified by the Surface Profile (the section view of Oblique Plot) in the range of 0.05~0.1μm.

After silicon nitride A in rolling contact with Type 2 steel balls for 125.59 hours (169.5 million stress cycles), the rolling track can hardly be seen under microscope with bright field. Fig. 6 A2 is the rolling track under microscope with dark field. The rolling track can only be recognised by contrast in colour. No oil deposit can be found at the edges of the rolling track.

*3.2 Silicon nitride B in rolling contact with Type 1 and Type 2 steel balls*

Silicon nitride B are with an average $R_a$ value 0.020 μm and a $\Delta_q$ value (root mean square value of average slope) 0.4˚.  After 100.72 hours RCF test (135 million stress cycles) with Type 1 steel balls, under optical microscopy observation (Fig. 6  B1) the surface pitting appears on the rolling track and the sides of the rolling track have become smoother. To verify this, a Scanning Electron Microscopy (SEM) investigation was carried out. Fig. 8  shows the SEM micrographs of sample B1, (a) and (b) outside the rolling track, (c) and (d) inside the rolling track. The SEM investigation leads to an assumption that during the rolling contact test, the vast majority of the small and shallow pits disappeared due to the  "polishing" wear process and the surface became smoother. However, some of the larger and deeper pits developed into surface pitting due to microcracking.

After silicon nitride B in rolling contact with Type 2 steel balls for 102.85 hours (139 million stress cycles),  no wear can be observed on the rolling track under microscope, only oil deposited at the rolling track edges, as shown in Fig. 6 B2.  In order to verify this, a 3D topography analysis was conducted on the rolling track. Fig. 9 is the analysis result, and wear can not be seen in the 3D Oblique Plot. From the Surface Profile of Fig. 9,  the hight of the oil residuals at the right edge of the rolling track is about 0.2 μm.

*3.3 Silicon nitride C in rolling contact with Type 1 and Type 2 steel balls*

Silicon nitride C are with an average $R_a$ value 0.002 μm. After 110.48 hours RCF test (149 million stress cycles) with Type 1 steel balls, the rolling track surface of C1 became rougher under optical microscopy observation (Fig. 6 C1). Oil residuals have deposited on both rolling track edges, with some black oil residuals on the inner edge in the width of 0.1mm. Fig. 10 shows the rolling track of sample C1 examined by the 3D surface analyzer. The amount of wear and the height of the oil deposits are similar to sample A1. A further 3D surface analysis on the black area of the rolling track confirms the black thing is oil stain with a height of 0.2~0.3 μm (Fig 11).

For silicon nitride C with Type 2 steel balls, three tests were conducted. Sample C2-1 failed with a fatigue spall after 21.94 hours (29.6 million stress cycles) as shown in Fig. 6 C2-1. This spall was examined by the 3D surface analyzer, and the result is shown in Fig. 12. The diameter of the spall is about 200 μm, and the deepest inside the spall is about 40 μm. Delamination occurred adjacent to the spall along the rolling track, a 3D surface analysis shows the depth of the delamination is about 0.8~1 μm (Fig. 13).

To examine if this spall failure for silicon nitride C in rolling contact with Type 2 steel balls is inevitable, another two more tests were conducted. Sample C2-2 tested for 128.42 hours (173 million stress cycles). After test, wear can be observed on the rolling track under microscope, and some small pittings in the dimension of 20~40 μm also appeared on the rolling track (Fig. 6 C2-2). Fig. 14 shows the interference profilometry image of the outer edge of the rolling track. A narrow oil deposit zone is near the edge of the rolling track, and immediate outside the oil deposit zone is a deep groove. Wear can also be seen inside the rolling track.

Sample C2-3 tested for 44.66 hours (60 million stress cycles). After test, wear can be observed on the rolling track under microscope. The wear is located near the centre of the rolling track, in the range of 0.15~0.2 μm as measured by 3D surface analysis (Fig. 15), which is severe than samples A1 and C1.


*3.4 Silicon nitride D in rolling contact with Type 1 and Type 2 steel balls*

Silicon nitride D are with an average $R_a$ value 0.002 μm and an average $R_q$ value 0.003 μm, which are the same as samples C. But silicon nitride D are with a high positive skewness value $R_{sk}$ of 3.1 and a very high kurtosis value $R_{ku}$ of 34.7, which means that the surfaces of D have more peaks than valleys and are "spiky". After 131.85 hours (177 million stress cycles), no difference can be observed on the rolling track of sample D1 except for oil stains at the track edges under optical microscopy (Fig. 6 D1). The high skewness and kurtosis values did not make any difference. The interference profilometry image in Fig. 15 shows the oil stain at the outer edge of the track. Small and shallow pitting around 2μm in size was observed on the rolling track of sample D1 with the SEM as shown in Fig. 17.

For Silicon nitride D in rolling contact with Type 2 steel balls for 102.85 hours (139 million stress cycles), rolling track can hardly be recognised under microscopy, as shown in Fig. 6 D2.

## 4. Discussion

*4.1 The effects of silicon nitride surface topography on RCF performance*

Four kinds of HIPed silicon nitride with surface roughness value $R_a$ ranging 0.002~0.016 μm were tested. No obvious correlation between the shape of surface topography and the rolling contact fatigue performance or rolling wear of HIPed silicon nitride can be found. For example, although the surface roughness values of samples A and samples D are in the same order (A with $R_a$ 0.004 μm and $R_q$ 0.006 μm, D with $R_a$ 0.002 μm and $R_q$ 0.003 μm), the surface topography of samples A and samples D are very different. Samples A are with an average negative skewness value –1.8 (the surface has more valleys than peaks), which are also revealed by the average $R_v$ (the maximum depth of the profile below the mean line) value of 0.048 μm. In contrast, samples D surfaces are "spiky" (have more peaks than valeys), which are indicated by a high positive skewness value $R_{sk}$ of 3.1 and a very high kurtosis value $R_{ku}$ of 34.7, and also disclosed by a high average $R_p$ (the maximum height of the profile above the mean line) value of 0.030 μm and a low average $R_v$ value of 0.009 μm. After RCF tests, no difference can be observed on the rolling tracks under microscope (Fig. 6 A1, A2, D1, D2). The wear on the rolling tracks were very small as measured by an analytical balance, in the range of 0.1 mg ~ 1mg. If this is converted to volume loss, it would be in the range of $0.3 \sim 3 \times 10^{-10}$ m$^3$. The amount of wear examined by 3D surface analysis (Fig. 7) and SEM (Fig. 17) were also very small.

The effect of another surface topography parameter $\Delta_q$ (root mean square value of average slope) was also not apparent during this study, although it was generally considered to be related to friction and wear properties. Samples B have a high $\Delta_q$ value of 0.4˚. After in rolling contact with Type 2 steel balls for 102.85 hours (139 million stress cycles), no wear can be observed on the rolling track under microscopy (Fig. 6 B2) or under 3D topography analysis (Fig. 9). But after samples B in rolling contact with Type 1 steel balls, surface pitting and polishing wear occurred (Fig 6 B1). This is related to the λ (lambda) ratio in EHD lubrication. It seems that $R_a$ or $R_q$ are still most important surface topography parameters (there is a linear relationship between $R_a$ and $R_q$, for a lapped surface, $R_a$ : $R_q$ can be 1:1.5 [13] ), because $R_q$ defines the composite surface roughness, which in turn determines the the λ (lambda) ratio. This will be discussed next.

*4.2 The effects of composite surface roughness and λ (lambda) ratio in EHD lubrication*

In Elastohydrodynamic Lubrication theory [12], the lubrication regime (lambda ratio) is found from the ratio of minimum film thickness to composite surface roughness,

$$\lambda = h_{min}/\sigma \tag{2}$$

where σ is composite surface roughness, and $h_{min}$ is the minimum film thickness, which is defined by the load, speed, materials and geometry of the two contacting surfaces, as well as lubricant viscosity.

$$\sigma = \sqrt{\left(R_{q1}^2 + R_{q2}^2\right)} \tag{3}$$

$R_{q1}$ and $R_{q2}$ are the rms roughness values for the two contacting surfaces. According to Elastohydrodynamic Lubrication theory, if $\lambda>3$, a full fluid film will separate the two surfaces, if $1<\lambda<3$, some asperities contact will occur.

The calculated minimum film thickness and lambda ratio for four kinds of HIPed silicon nitride in rolling contact with two types of steel are listed in Table 5. The EHD theory is well proved in this study. The λ (lambda) ratio for sample B1 is 2.69. This means that the lubrication film will not fully separate the two contact surfaces, and some asperities contact will occur. This explains the polishing wear and surface pitting on the rolling track of B1 observed by microscope and SEM. It is also very interesting to notice that when the λ (lambda) ratio is just above 3, there are oil deposit at the edges of the rolling track (samples A1, B2, C1, D1). When the λ (lambda) ratio is much greater than 3, there are no oil deposit at the edges of the rolling track (samples A2, D2). So the oil deposit may be related to the λ (lambda) ratio as well. For samples C2, the situations are complicated and will be discussed next.

*4.3 The effects of steel surface hardness and roughness on the RCF performances of silicon nitride*

For silicon nitride C in rolling contact with Type 1 steel, the amount of wear on the rolling track is comparable to Sample A1 as measured by 3D surface analyzer (Fig. 10). The rolling track is not as clean as other samples (Fig. 6 C1), and black oil stain deposited on the rolling track (Fig. 11). For silicon nitride C in rolling contact with Type 2 steel, C2-1 failed with a fatigue spall after 29.6 million stress cycles. This failure may be probabilistic, or due to an undetected pre-existed surface defect (flaw) on the rolling track. Two more RCF tests on silicon nitride C in rolling contact with Type 2 steel were conducted, and no further fatigue spall was found. To conduct a reasonable probabilistic failure analysis, at least 20 tests were needed for each kind of samples, and this is beyond the scope and capability of current study. But the further two RCF tests on C2 did show some differences on the rolling tracks, compared with similar surface roughness samples A2 and D2, and compared with the same surface but in rolling contact with Type 1 steel (C1). For Sample C2-2 after 173 million stress cycles, wear and surface pittings can be seen on the rolling track (Fig. 6 C2-2), and interference profilometry image revealed a groove at the edge of the rolling track (Fig. 14). For Sample C2-3 after 60 million stress cycles, wear on the rolling track is severe than samples A1 and C1, as measured by 3D surface analyzer (Fig. 15).

There is a possibility that a kind of "affinity" exist between silicon nitride C and the testing steel (Type 1 and Type2 steel balls are supposed to have the same composition but with different hardness and surface roughness). Although samples A to D are all HIPed silicon nitride, they were manufactured by different manufacturers, and different additives may be added during the manufacturing processes. Thus they may have different chemical properties. Although there is a very thin fluid film separate the two surfaces, this "affinity" accelerated the tribochemical reaction between the two surfaces. This is why the rolling track of C1 is not as clean as other samples, and black oil stain deposited on the rolling track. When the surface hardness ratio and surface roughness ration of the two contacting surfaces are within certain range, this "affinity" can be most activating. Thus, the probabilistic fatigue spall occurred on C2-1, and severe wear on the rolling tracks of C2-2 and C2-3 took place. This is only an assumption, and to prove it detailed chemical

analysis is needed. However, a suggestion could be drawn from this study is that the best possible surface finishing on silicon nitride may not consequently lead to best RCF performance, there are many other influencing factors. A previous study on silicon nitride/steel contact by Lakshminarayanan and Chao also showed the as-ground silicon nitride exhibited better RCF performance than the ground-and-lapped silicon nitride [6].

*4.4 The effect of steel surface hardness and roughness on failure time in rolling contact with silicon nitride*

The surface hardness of Type 1 steel is only 4.5% higher in HV readings, and 1.24% in HRC readings than Type 2 steel. The surface roughness values of $R_a$ and $R_q$ are higher for Type 1 steel balls than Type 2 steel balls. The average fatigue life for Type 1 steel is 43.4 hours, whilst the average fatigue life for Type 2 steel is 10.77 hours. It is unlikely that the lower $R_a$ and $R_q$ values of Type 2 steel balls could greatly reduce their RCF life, because previous reports both showed that higher $R_q$ value reduced the fatigue life of steel [4,5]. Since the contact stress is high and beyond the elastic limit of steel balls (regardless of Type 1 or Type 2) but lower than that of ceramic balls, the steel balls will shakedown [14] before settling in (after the running in stage due to microslip, or even in pure rolling contact). This shakedown will greatly reduce the effect of surface roughness of steel balls. It is more likely that the harness of steel played a significant role in the RCF life of steel in rolling contact with silicon nitride under lubricated condition. Although the actual contact geometry and stress conditions in hybrid ball bearings are very different form ball/ball contact in this study, the experiment results could be used as a clue to improve the RCF life of steel raceway.

## 5. Conclusion

Four kinds of HIPed silicon nitride with different surface roughness parameters were rolling against two types of steel in fully lubricated condition under high speed (10,000 rpm) and high contact stress (6.58 GPa) for 135~180 million stress cycles. After tests, the rolling track surfaces were examined by optical microscope, SEM, 3-D surface structure analyzer and interference profilometer. Experiment results can be summarised as following:

(1) The composite surface roughness determined by $R_q$ values of both steel and silicon nitride, are most influential in lubricated rolling contact fatigue.

(2) The shape of the surface topography of silicon nitride, like $R_{sk}$, $R_{ku}$, $R_p$, $R_v$ and $\Delta_q$, are not sensitive in this study in relation to rolling contact fatigue performance.

(3) The best possible surface finishing on silicon nitride may not consequently lead to best RCF performance, and there are many other influencing factors including a possibility of "affinity" between silicon nitride and steel.

(4) The slight difference in steel surface hardness may lead to significant differences in fatigue life of steel in rolling contact with silicon nitride.

**References:**

[1] Cundill RT. High-precision silicon nitride balls for bearings, Vol.1573, Int Soc for Optical Engineering, Bellingham, WA, USA, 1992. p. 75-86.

[2] Wang L, Snidle RW, Gu L. Rolling contact silicon nitride bearing technology: a review of recent research. Wear 2000; 246 159-173.

[3] Scott D , Blackwell J. Study of the effect of material combination and hardness in rolling contact. Proceedings of Institute of Mechanical Engineers 1966; 180 (3K): 32-36.

[4] Tourret R, Wright EP, Rolling contact fatigue: Performance testing of lubricants, Heyden & Son LTD, 1977.

[5] Tallian TE. A data-fitted rolling bearing life prediction model-Part II: Model fit to the historical experimental database. Tribology Transactions 1996; 39 (2): 259-268.

[6] Lakshminarayanan R, Chao LY, Iyer N, Shetty DK. Wear of steel in rolling contact with silicon nitride. Wear 1997; 210 (1-2): 278-286.

[7] Effner U, Woydt M. Importance of machining on tribology of lubricated slip-rolling contacts of $Si_3N_4$, $SiC$, $Si_3N_4$-$TiN$ and $ZrO_2$. Wear 1998; 216 (2): 123-130.

[8] Westkaemper E , Hoffmeister HW. Function-oriented surface characterization of lapped and polished  ceramic rolling elements. In: 7th Int. Conf. on Metrology and Properties of Engineering Surfaces, 1997. p. 432-443.

[9] Chao LY, Lakshminarayanan R, Iyer N, Lin GY, Shetty DK. Transient wear of silicon nitride in lubricated rolling contact. Wear, 1998; 223 (1-2): 58-65.

[10] Kang J, Hadfield M. The influence of heterogeneous porosity on silicon nitride/steel wear in lubricated rolling contact. Ceramics International 2000; 26 (3): 315-324.

[11] Johnson KL. Contact Mechanics, Cambridge University Press, 1985.

[12] Dowson D, Higginson GR. Elasto-Hydrodynamic Lubrication, Pergamon Press, 1966.

[13] Dagnall H. Exploring surface texture, Rank Taylor Hobson Limited, 1986.

[14] Kapoor, A, Williams, JA. Shakedown limits in rolling-sliding point contacts on an anisotropic half space, Tribology International 1996; 191(1-2); 256-260.

**List of Tables and Figures**

| Samples | Diameter mm | Surface roughness $R_a$ μm (average) | Density $(kg/m^3)$ | Surface Hardness (HV10) |
|---------|-------------|--------------------------------------|--------------------|--------------------------|
| A | 12.7004 | 0.004 | 3214 | 1505 |
| B | 12.7007 | 0.020 | 3238 | 1560 |
| C | 12.6994 | 0.002 | 3226 | 1478 |
| D | 12.6998 | 0.002 | 3166 | 1619 |

Table 1  The measured geometric and material properties of HIPed $Si_3N_4$ samples

| | Steel Testing Ball Type 1 | Steel Testing Ball Type 2 |
|---|---|---|
| Diameter | 12.699 mm | 12.700 mm |
| Density | 7789 $(kg/m^3)$ | 7781 $(kg/m^3)$ |
| Surface roughness $R_a$ | 0.024 μm | 0.0108 μm |
| Surface roughness $R_q$ | 0.037 μm | 0.0172 μm |
| Surface Hardness | 907 (HV10) | 868 (HV10) |
| Surface Hardness | 65.2 HRC-150kg | 64.4 HRC-150kg |

Table 2 The measured geometric and material properties of two kinds of steel balls

| Test Number | Silicon nitride sample | Steel samples | Total RCF test duration (hours) | Total contact stress cycles (million) | Lower balls changed after (hours) | Final temperature ( °C ) | Test termination and observations |
|---|---|---|---|---|---|---|---|
| A1 | A | Type 1 | 134.35 | 181.3725 | 17.083, 49.867, 67.4 | 63.8 | Oil residues on upper ball |
| A2 | A | Type 2 | 125.59 | 169.5465 | 6.83, 18.2, 7.7, 16.62 9.08, 8.32, 7.63, 10.58, 4.47, 7.62, 10.47, 7.92, 10.15 | 61.3 | One lower ball small spall |
| B1 | B | Type 1 | 100.72 | 135.972 | 39.68, 10.2, 50.84 | 62.2 | One lower ball small spall, small amount of dark debris in oil |
| B2 | B | Type 2 | 102.85 | 138.8475 | 14.95, 10.55, 1.1, 7.28, 22.85, 9.1, 8.37, 5.95, 11.1, 11.6 | 62.2 | One lower ball spall |
| C1 | C | Type 1 | 110.48 | 149.148 | 8.07, 102.41 | 65.6 | Oil residues on upper ball |
| C2-1 | C | Type 2 | 21.94 | 29.619 | 8.42, 6.77, 5.92, 0.83 | 59.8 | Upper silicon nitride sample ball spall |
| C2-2 | C | Type 2 | 128.42 | 173.367 | 29.46, 18.82, 25.5, 13.83, 17.73, 23.08 | 64.2 | One lower ball spall |
| C2-3 | C | Type 2 | 44.66 | 60.291 | 6.17, 9, 5.65, 9.22, 14.62 | 60.5 | One lower ball spall |
| D1 | D | Type 1 | 131.85 | 177.9975 | 22.57, 8.91, 100.37 | 64.2 | Oil residues on upper ball, Some rust-like ebris in the oil at the bottom of the retainer cup |
| D2 | D | Type 2 | 114.64 | 154.764 | 6.82, 10.7, 9.48, 9.23, 9.85, 7.5, 10.93, 14.05, 13.17, 9.22, 6.28, 7.95 | 64.2 | One lower ball spall |

Table 3 Rolling contact fatigue test records

| PLINT Machine Load (KN) | 1.96 |
|---|---|
| Contact Load (N) | 800 |
| Max. Compressive Stress (GPa) | 6.58 |
| Radius of Contact Circle (mm) | 0.24 |
| Max. Shear Stress (GPa) | 2.04 |
| Max. Tensile Stress (GPa) | 1.01 |

Table 4  The calculated Hertz contact stresses

| Samples | $R_{q1}$ (µm) ceramic | $R_{q2}$ (µm) steel | $h_{min}$ (µm) | $\lambda$ |
|---|---|---|---|---|
| A1 | 0.006 | 0.0376 | 0.125 | 3.27 |
| A2 | 0.006 | 0.0172 | 0.125 | 6.84 |
| B1 | 0.027 | 0.0376 | 0.125 | 2.69 |
| B2 | 0.027 | 0.0172 | 0.125 | 3.89 |
| C1 | 0.003 | 0.0376 | 0.125 | 3.31 |
| C2 | 0.003 | 0.0172 | 0.125 | 7.14 |
| D1 | 0.003 | 0.0376 | 0.125 | 3.31 |
| D2 | 0.003 | 0.0172 | 0.125 | 7.14 |

Table 5 The calculated minimum film thickness and lambda ratio

**A** (ID: 8)

| ROUGHNESS – ISO | | S | X̄ | X MAX | X MIN | LAST X |
|---|---|---|---|---|---|---|
| Ra | µm | 0.000 | 0.004 | 0.005 | 0.004 | 0.004 |
| Rq | µm | 0.001 | 0.006 | 0.007 | 0.005 | 0.005 |
| Ry | µm | 0.021 | 0.068 | 0.087 | 0.045 | 0.045 |
| Rtm | µm | 0.013 | 0.049 | 0.058 | 0.035 | 0.035 |
| Rv | µm | 0.016 | 0.048 | 0.063 | 0.031 | 0.031 |
| Rp | µm | 0.003 | 0.022 | 0.023 | 0.018 | 0.018 |
| Sm | µm | 1 | 25 | 26 | 25 | 25 |
| λq | µm | 3 | 25 | 27 | 23 | 27 |
| Δq | ° | 0.0 | 0.1 | 0.1 | 0.1 | 0.1 |
| Rsk | | 0.6 | -1.8 | 0.0 | -2.1 | -1.1 |
| Rku | | 4.7 | 11.2 | 15.4 | 6.1 | 6.1 |
| S | µm | 0 | 13 | 13 | 13 | 13 |
| R3z | µm | 0.005 | 0.030 | 0.033 | 0.024 | 0.024 |
| Rpm | µm | 0.002 | 0.014 | 0.016 | 0.012 | 0.012 |
| R3y | µm | 0.005 | 0.037 | 0.041 | 0.031 | 0.031 |

0-EXCLUDE LAST X    N= 3 OF 3

**B** (ID: 15)

| ROUGHNESS – ISO | | S | X̄ | X MAX | X MIN | LAST X |
|---|---|---|---|---|---|---|
| Ra | µm | 0.003 | 0.020 | 0.023 | 0.016 | 0.023 |
| Rq | µm | 0.007 | 0.027 | 0.034 | 0.020 | 0.034 |
| Ry | µm | 0.099 | 0.213 | 0.314 | 0.116 | 0.314 |
| Rtm | µm | 0.081 | 0.179 | 0.263 | 0.102 | 0.263 |
| Rv | µm | 0.077 | 0.155 | 0.226 | 0.074 | 0.226 |
| Rp | µm | 0.070 | 0.089 | 0.169 | 0.047 | 0.169 |
| Sm | µm | 4 | 29 | 32 | 25 | 29 |
| λq | µm | 4 | 28 | 33 | 25 | 25 |
| Δq | ° | 0.1 | 0.4 | 0.5 | 0.2 | 0.5 |
| Rsk | | 0.8 | -1.3 | 0.0 | -1.8 | -1.6 |
| Rku | | 3.3 | 6.8 | 8.9 | 3.0 | 8.9 |
| S | µm | 1 | 15 | 16 | 13 | 16 |
| R3z | µm | 0.041 | 0.126 | 0.165 | 0.084 | 0.165 |
| Rpm | µm | 0.024 | 0.056 | 0.083 | 0.042 | 0.083 |
| R3y | µm | 0.047 | 0.151 | 0.188 | 0.098 | 0.188 |

0-EXCLUDE LAST X    N= 3 OF 3

**C** (ID: 11)

| ROUGHNESS – ISO | | S | X̄ | X MAX | X MIN | LAST X |
|---|---|---|---|---|---|---|
| Ra | µm | 0.000 | 0.002 | 0.002 | 0.002 | 0.002 |
| Rq | µm | 0.000 | 0.003 | 0.003 | 0.003 | 0.003 |
| Ry | µm | 0.016 | 0.047 | 0.065 | 0.036 | 0.041 |
| Rtm | µm | 0.001 | 0.027 | 0.028 | 0.026 | 0.028 |
| Rv | µm | 0.004 | 0.027 | 0.030 | 0.022 | 0.030 |
| Rp | µm | 0.023 | 0.028 | 0.054 | 0.012 | 0.012 |
| Sm | µm | 5 | 29 | 34 | 25 | 25 |
| λq | µm | 2 | 27 | 28 | 25 | 25 |
| Δq | ° | 0.0 | 0.0 | 0.0 | 0.0 | 0.0 |
| Rsk | | 2.7 | 0.2 | 3.2 | -1.7 | -1.7 |
| Rku | | 30.2 | 29.4 | 64.1 | 9.6 | 14.5 |
| S | µm | 1 | 14 | 15 | 13 | 13 |
| R3z | µm | 0.002 | 0.014 | 0.016 | 0.013 | 0.016 |
| Rpm | µm | 0.004 | 0.011 | 0.016 | 0.008 | 0.008 |
| R3y | µm | 0.004 | 0.018 | 0.023 | 0.014 | 0.023 |

0-EXCLUDE LAST X    N= 3 OF 3

**D** (ID: 18)

| ROUGHNESS – ISO | | S | X̄ | X MAX | X MIN | LAST X |
|---|---|---|---|---|---|---|
| Ra | µm | 0.000 | 0.002 | 0.002 | 0.001 | 0.001 |
| Rq | µm | 0.001 | 0.003 | 0.004 | 0.002 | 0.002 |
| Ry | µm | 0.017 | 0.038 | 0.057 | 0.025 | 0.025 |
| Rtm | µm | 0.002 | 0.021 | 0.023 | 0.020 | 0.021 |
| Rv | µm | 0.001 | 0.009 | 0.010 | 0.008 | 0.008 |
| Rp | µm | 0.016 | 0.030 | 0.048 | 0.017 | 0.017 |
| Sm | µm | 22 | 44 | 65 | 22 | 22 |
| λq | µm | 11 | 34 | 47 | 25 | 25 |
| Δq | ° | 0.0 | 0.0 | 0.0 | 0.0 | 0.0 |
| Rsk | | 1.9 | 3.1 | 5.3 | 2.0 | 2.0 |
| Rku | | 25.7 | 34.7 | 64.2 | 18.1 | 18.1 |
| S | µm | 3 | 15 | 19 | 13 | 13 |
| R3z | µm | 0.000 | 0.009 | 0.010 | 0.009 | 0.009 |
| Rpm | µm | 0.002 | 0.015 | 0.016 | 0.013 | 0.015 |
| R3y | µm | 0.001 | 0.012 | 0.012 | 0.011 | 0.011 |

0-EXCLUDE LAST X    N= 3 OF 3

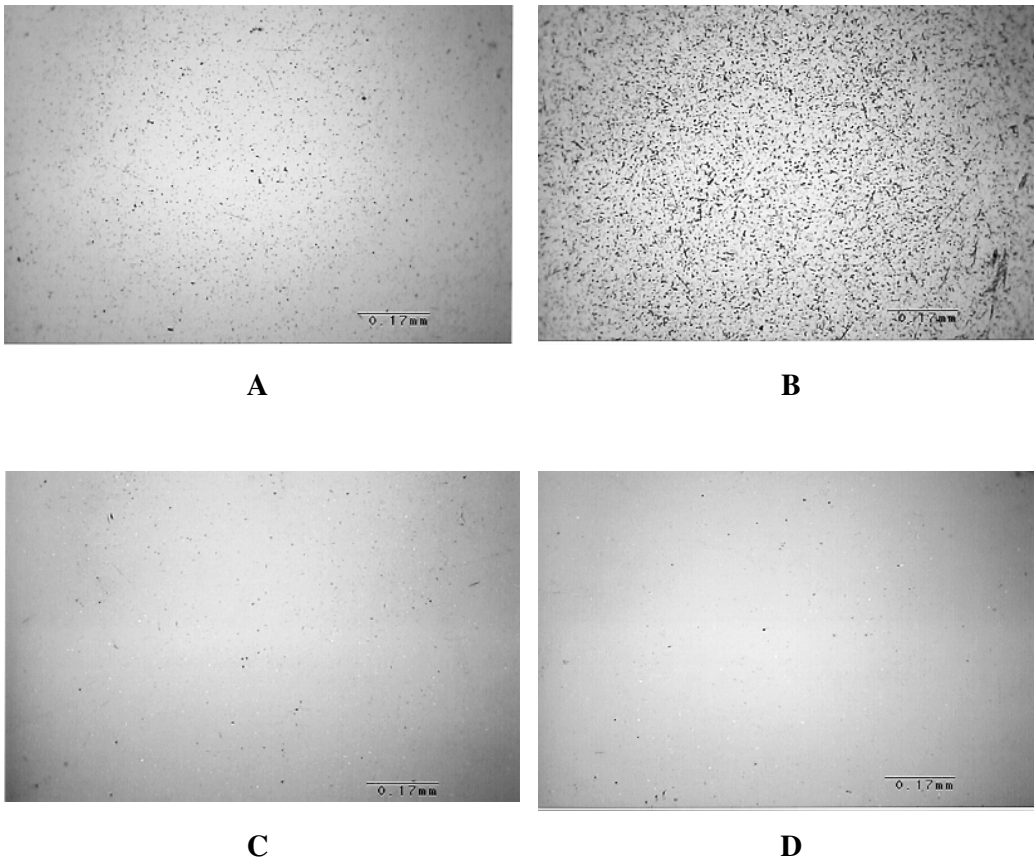Fig. 1  2D statistical analysis of HIPed $Si_3N_4$ sample surfaces A to D before testing.

Fig. 2 Photomicrographs of the HIPed $Si_3N_4$ surfaces of samples A to D before testing.
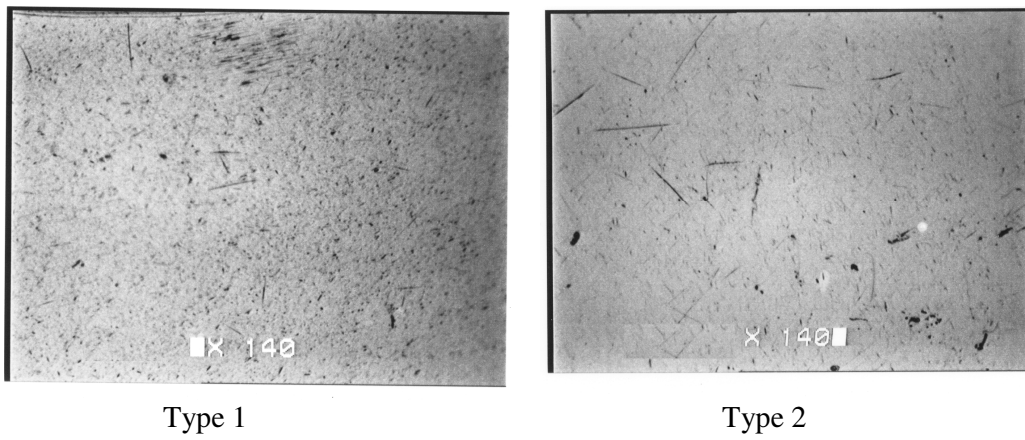


Fig. 3 Photomicrographs of the surfaces of two types of steel testing balls
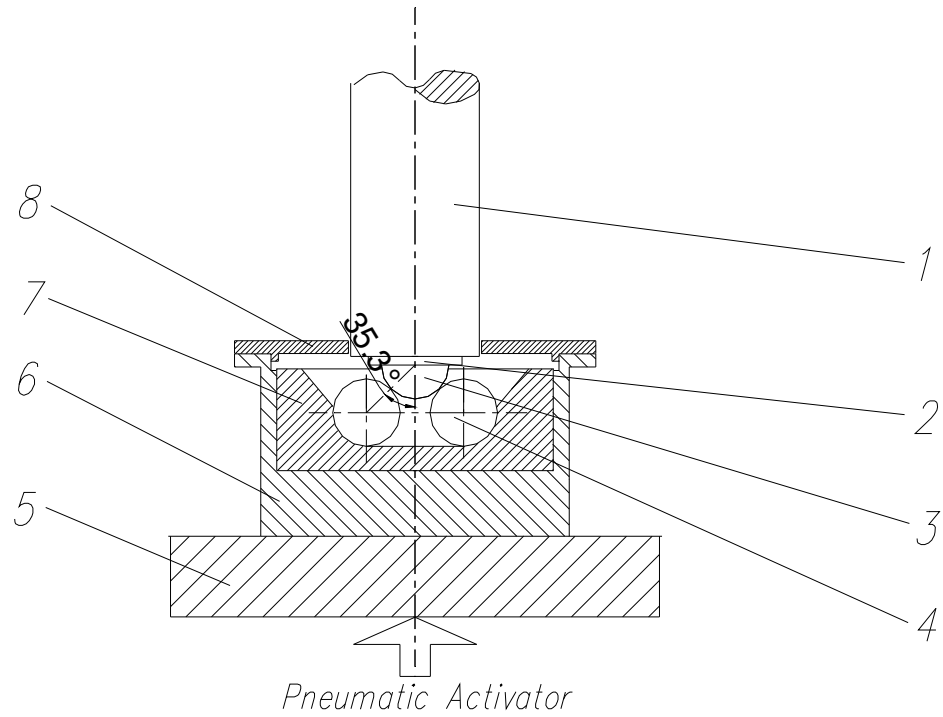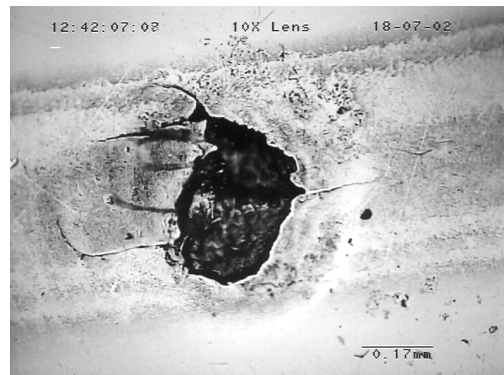
Fig. 4 Schematic of the modified four-ball rolling configuration
1 spindle      2 collet      3 upper-ball      4 lower-balls      5 heater pad
6 cup holder      7 retainer cup      8 cup cover



(a)                                    (b)
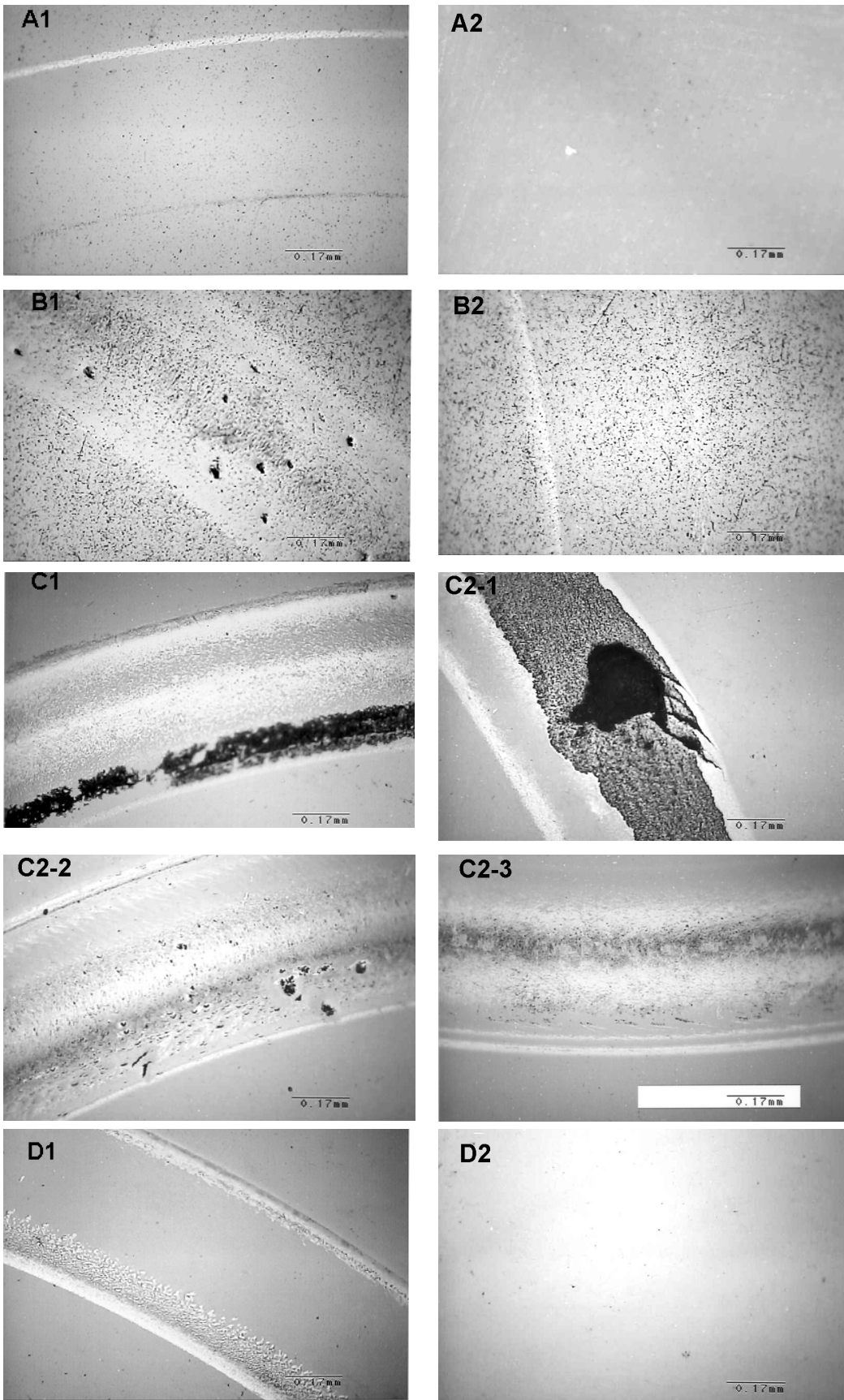
Fig. 5 Typical big and small fatigue spalls on steel balls

Fig. 6 Photomicrographs of the rolling tracks of samples A to D after testing.
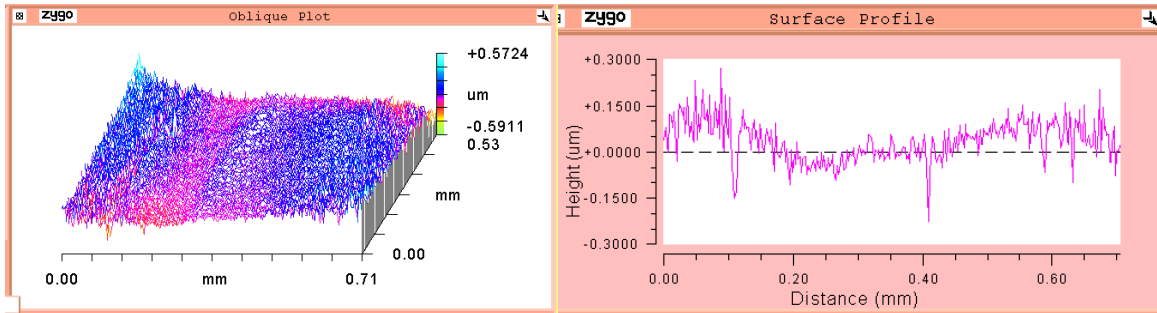
Fig. 7 Rolling wear track of sample A1 observed by 3D surface analysis



(a)

(b)

(c)

(d)
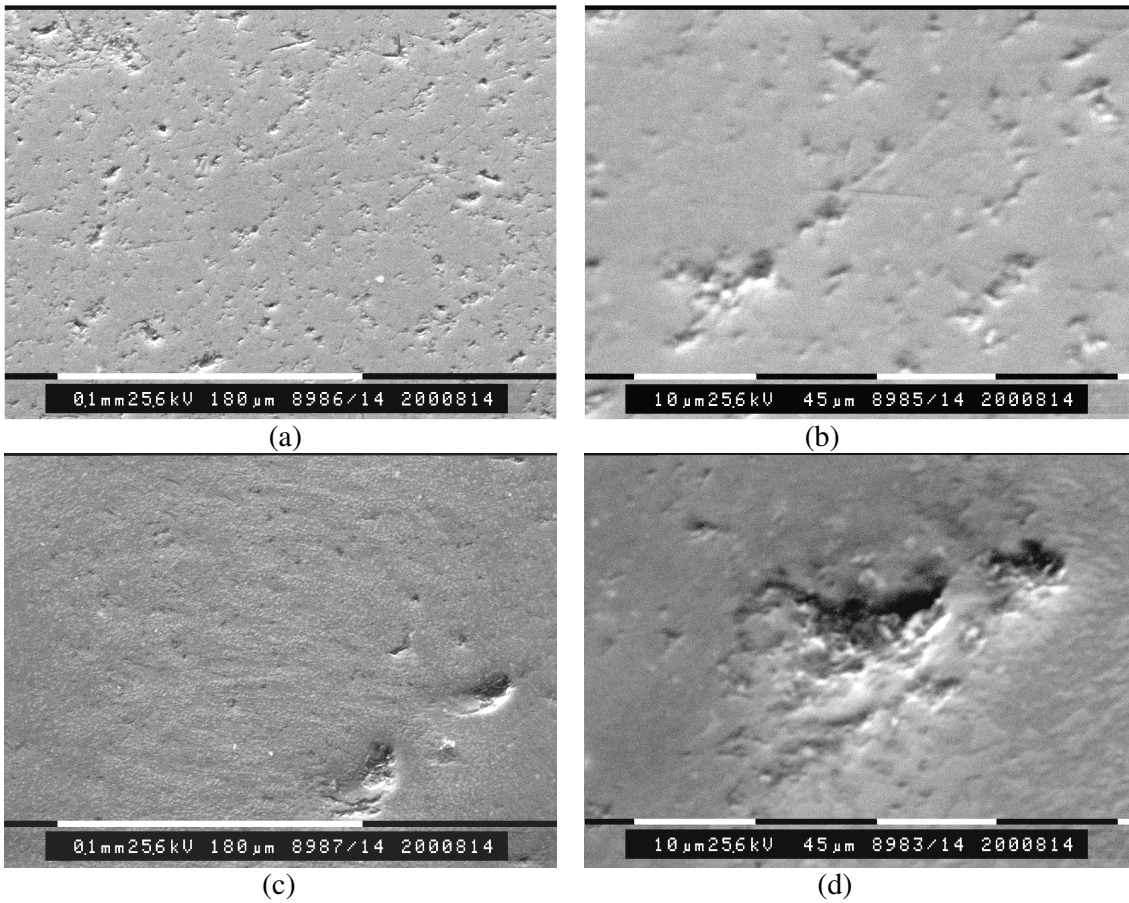
Fig. 8   SEM micrographs of sample B1,
(a) and (b) outside the rolling track, (c) and (d) inside the rolling track.
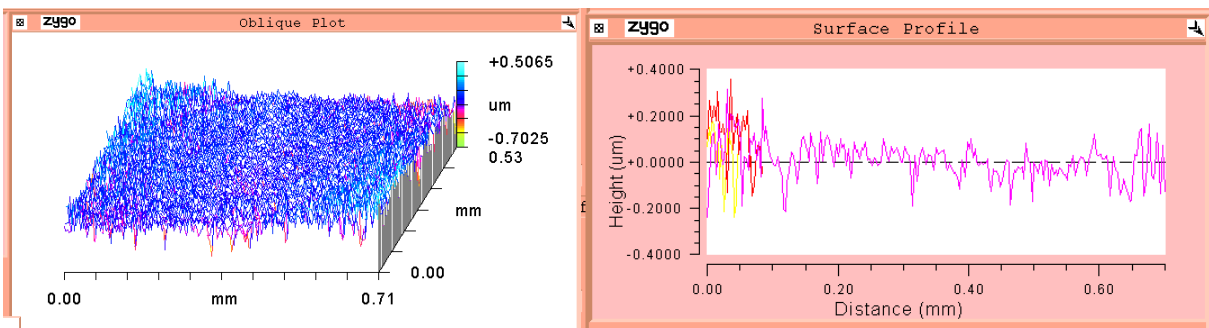


Fig. 9 Rolling track of sample B2 observed by 3D surface structure analysis
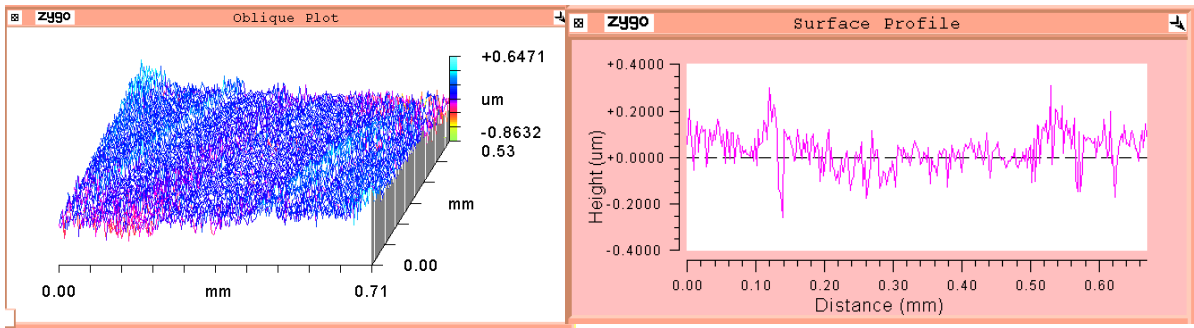
Fig. 10 the rolling track of sample C1 examined by the 3D surface analyzer.
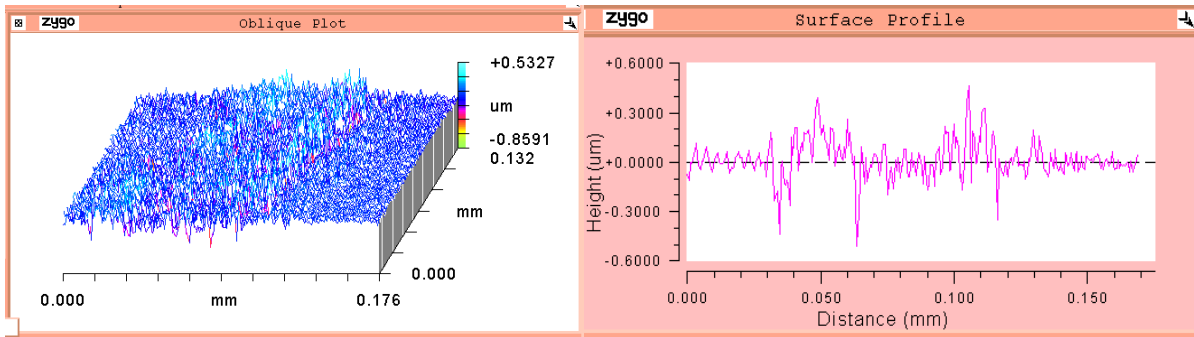


Fig. 11 the black area of sample C1 examined by the 3D surface analyzer.
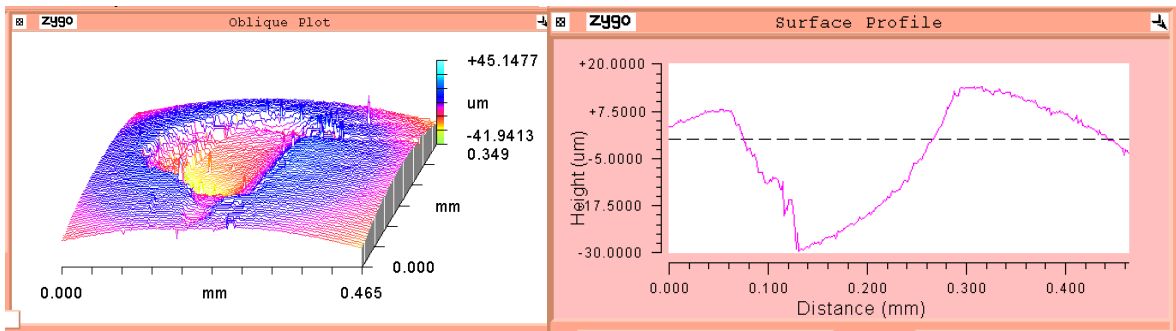


Fig. 12  Rolling track of sample C2-1 observed by 3D surface analysis
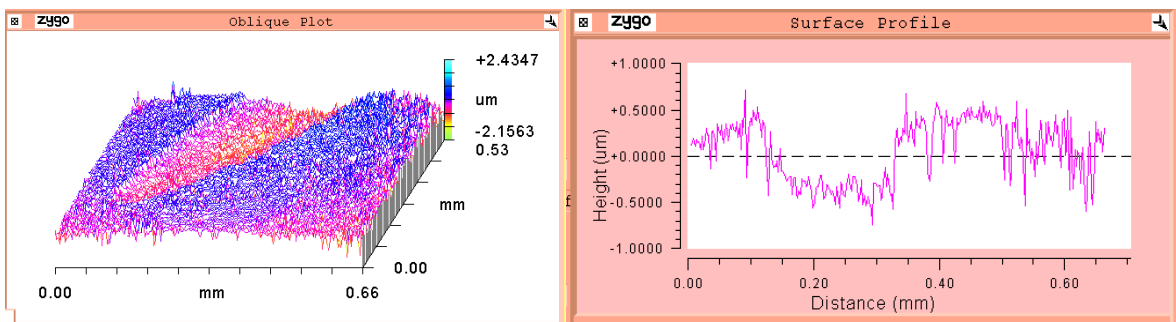


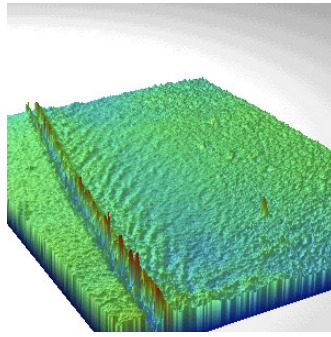Fig. 13  Delamination on the  Rolling track of sample C2-1 measured by 3D analysis

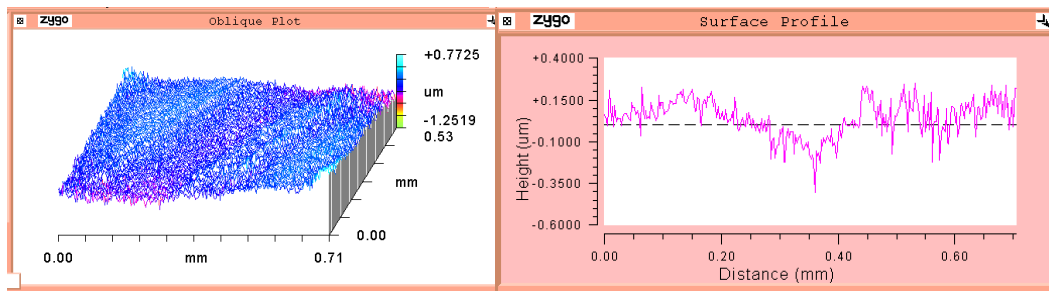Fig. 14 The interference profilometry images of the rolling tracks of samples C2-2.



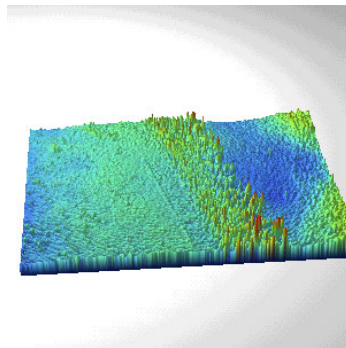Fig. 15 Rolling track of sample C2-3 observed by 3D surface structure analysis.



Fig. 16 The interference profilometry image of the rolling track of sample D1.



Fig. 1**7** Small pitting on the rolling track of sample D1 observed by SEM.